# Characterisation of Residual Stress in Electron Beam Welded P91 Plates by Neutron Diffraction

**Amrita Kundu[1,*], Peter John Bouchard[1], Santosh Kumar[2], Gautam Kumar Dey[2]**

[1]Materials Engineering, The Open University, Milton Keynes, MK7 6AA, UK
[2]Materials Science Division, BARC, Mumbai, India

**Abstract**  This paper describes the characterisation of residual stress in electron beam welded P91 ferritic-martensitic steel plates (9 mm thick) by neutron diffraction. The novelty of the work lies in revealing the residual stress profile at a fine length scale associated with a ~ 1 mm wide fusion zone. A characteristic 'M' shaped distribution of stresses across the weld line is observed with high tensile peaks situated just beyond the HAZ/parent material boundary. Measured stresses close to the weld centre-line are significantly less tensile than the adjacent peaks owing to martensitic phase transformation during cool-down of the weld region. The effect of applying a second smoothing electron beam weld pass is shown to be undesirable because it increases the tensile magnitude and spread of residual stress.

**Keywords**  Electron Beam Weld, Residual Stress, Ferritic Martensitic Steel, Neutron Diffraction

## 1. Introduction

Ferritic-martensitic steels containing 9-12 Cr are seen as offering the most promise for components such as headers and the main steam pipe in ultra-supercritical (USC) fossil-fired power plants, as well as for primary components in some of the design concepts for Generation IV nuclear reactors[1]. This is because 9-12 Cr steels offer superior creep strength to grades containing less chromium such as, for example, 2.25Cr-1Mo steels. Steels containing 9-12 Cr are also less expensive than austenitic stainless steels, and the fact that they have a higher thermal conductivity than austenitic steels means that they are less prone to the generation of thermal stresses when subjected to the thermal transients such as those that arise during plant outages and shut downs for scheduled maintenance.

While the advantages of 9-12 Cr steels are well recognized, the performance benefits often have not been realized in service operation due premature failures in the heat-affected zone (HAZ) of welded joints. The failure mechanism is type IV cracking[1], which refers to an enhanced rate of creep void formation in the fine-grained and intercritically-annealed HAZ of a weld. In recent years, significant efforts have been dedicated to understanding the influence that HAZ microstructures have in influencing the propensity for type IV failures in 9-12 Cr steels[1].

In this work we are focusing on modified P91 steel[2] as it is commercially available and currently in service. We wish to explore the influence that the choice of welding process might have in influencing the tendency for type IV failure. In particular, we have noted that there is some evidence to suggest that welds made with high-energy beam processes such as laser or electron beam welding may be more resistant to type IV cracking than welds made with conventional arc welding processes[1, 3]. It has been suggested that superior performance might be offered by laser- and electron-beam welds due to these processes generating a narrower HAZ than that for an arc welding process[1]. However, recent measurement work[1, 3] has also shown that when a P91 pipe girth weld was made with gas-tungsten arc (GTA) and submerged arc welding, substantial tensile residual stresses were generated in the type IV region. Moreover, these stresses were not entirely relieved by a conventional post-weld heat treatment (PWHT). It is possible, therefore, that residual stresses may also be contributing to type IV cracking in some way.

This article reports on the measurement of residual stresses in electron beam welds in a 9 mm thick P91 steel plate in the as-welded state. The purpose is to provide detailed characterisation of the residual stress field for validation of weld numerical models and to contribute to work investigating how the Electron Beam (EB) welding process influences the tendency for type IV cracking. Results for two plates are presented, with one containing a single pass weld and the other being made in two passes, that is a welding pass and a (cosmetic) smoothing pass. In this work, the residual stresses have been measured by neutron diffraction.

* Corresponding author:
akundu05@gmail.com (Amrita Kundu)

## 2. Experimental

**Table 1.**  Chemical composition of the steel (remaining Fe)

| C | Mn | Zr | Si | P | S | Cr | Mo | Ni | Cu | Al | N | Nb | Ti | V |
|---|----|----|----|----|----|----|----|----|----|----|----|----|----|----|
| 0.106 | 0.443 | 0.005 | 0.221 | 0.018 | 0.0008 | 8.965 | 0.901 | 0.212 | 0.045 | 0.010 | 0.0464 | 0.073 | 0.004 | 0.194 |

The base material studied in the present investigation is P91 steel having the chemical composition given in the Table 1. As-received hot-rolled plate material was first normalised at 1050 °C for 1min/mm and then tempered at 770 °C for 3 min/mm, followed by an air cool. Several plate samples of dimensions 245 mm by 145 mm were machined from the tempered material which was nominally 10 mm thick. The samples were then surface ground on both sides in order to remove a slight waviness of the plates originating from the hot rolling fabrication process. The final thickness of the plate material ranged from 9.2 mm to 9.8 mm.

Two pairs of surface ground plates were joined by an EB welding process with a voltage of 60 kV, current of 70 mA and welding speed of 1 m/min. No pre-heat was applied and the plates were spot welded along the seam. The plates were held rigidly using pneumatically controlled clamps during welding. An additional smoothing pass was applied to the second plate with a voltage of 60 KV and defocused beam current of 30 mA, again at a welding speed of 1 m/min. The as-welded residual stresses in both of these plates were studied by neutron diffraction supported by metallographic characterisation, as described below.

Cross sectional samples from the ends of both EB welded plates by electro-discharge machining (EDM). The samples were first ground using 400 grade Emery paper and then metallographically polished to a 1 μm finish. The macrostructure of the weld fusion zone was revealed by etching with Villela agent following which a hardness survey was undertaken using a measurement pitch of 0.5 mm and a Vickers indenter with a load of 0.3 kg.

Neutron diffraction residual stress measurements were carried out on the ENGIN-X beam-line at the ISIS facility of the Rutherford Appleton Laboratory in the UK. At this facility a spallation source is used to produce a "white" beam of variable wavelength neutrons. Time of flight is used to determine the lattice spacing in a gauge volume defined by sets of incoming slits and the capture angle of the detectors. Because of the very narrow width of the EB weld fusion zone, 1 mm detectors were mounted and used for all the measurements. The incoming beam was controlled by slits to give a (1x1x1) mm$^3$ gauge size for strains measured in the longitudinal direction and an extended gauge length of 10 mm for measurements in the transverse and normal directions. In each welded plate measurements were made through the thickness at the weld centre-line and along a line positioned 1.5 mm below the top surface of the plate. In the case of the plate, which received an additional smoothing pass, this 1.5 mm below line is at the interface between the two passes. The Rietveld refinement method[4] and General

Structure Analysis System software were used to analyse the measured spectra. It was ensured that the range of each spectrum selected for analysis contained at least 5 identifiable peaks from sets of crystallographic planes.

The lattice strain in a given direction is determined from the lattice spacing, $d$, measured at the location of interest, and the lattice spacing measured in representative (or ideally the same) material that is free from macroscopic stress; the latter quantity, the stress-free lattice parameter, is denoted as $d_0$. For direct strains in direction $i$ the strain $\varepsilon_{ii}$ is given by:

$$\varepsilon_{ii} = \frac{d_{ii} - d_{0ii}}{d_{0ii}}$$

If strains in three orthogonal directions are measured then the direct stresses, $S_{ii}$, can be determined using the following equation:

$$\sigma_{ii} = \frac{E}{(1+v)}\left[\varepsilon_{ii} + \frac{v}{(1-2v)}\left(\varepsilon_{ii} + \varepsilon_{jj} + \varepsilon_{kk}\right)\right]$$

Where $E$ is the bulk Young's modulus and $v$ is Poisson's ratio. In the present case $E = 218$ GPa and $v = 0.3$ were used for both the P91 base metal and fused zone[2].

A 2 mm thick strip was electro-discharge machined from the end of each plate and position dependent stress-free lattice parameter reference values, $d_0$, measured, relative to the weld centre-line and top surface, in order to take account of gradients in both the microstructure and strain history of the welded plates. For each point lattice parameters measurements were made in the longitudinal, transverse and the normal directions and an orientation independent lattice parameter determined assuming plane stress state conditions.

## 3. Results and Discussion

Figure 1(a) shows the macrostructure of a single pass EB welded plate, with the line along which the cross-weld hardness profile at 1.5mm was determined superimposed. The width of the fused zone tapers from 1.2mm at the top of the plate to about 0.8mm at the bottom. The width of the HAZ appears to extend about 0.8mm beyond the fusion boundaries on both sides. The hardness profile, Figure 1(c), matches the visible extent of the HAZ boundaries, rising rapidly from the parent material level of 230HV (at ± 1.3mm) to a plateau of about 480HV magnitude that spans the fusion zone. The plateau hardness level is indicative of a full martensitic microstructure which is seen to extend to a width of 1.4mm (slightly wider than the fused width of 1.1mm). The effect of applying a second smoothing EB weld pass is evident in Figure 1(b). Here the fusion boundary associated

with the second pass extends to a depth of about 1.5mm below the top surface. The maximum width of the second pass at the top surface is about 2.5mm. The hardness profile at 1.5mm depth is almost identical to the single EB welded case apart from being 0.2mm wider owing to the influence of the smoothing pass.



(a)



(b)



(c)
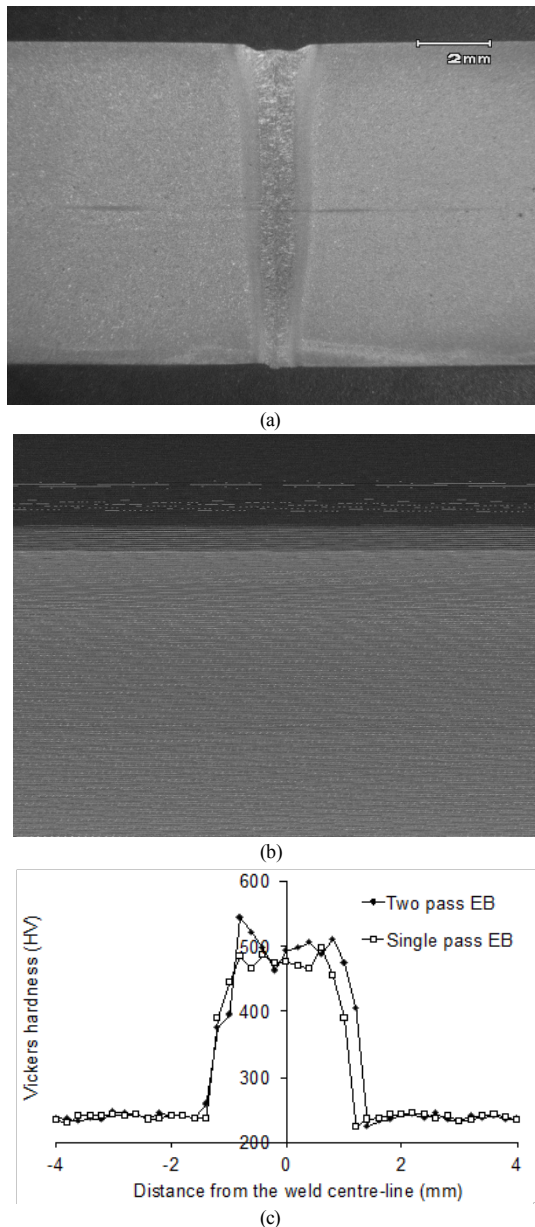
**Figure 1.** Photographs showing the macrostructure with superimposed measurement lines at 1.5 mm below the top surface of the weld for (a) the single pass EB welded plate and (b) the two pass (smoothed) EB welded plate

Figure 2 shows the variation in stress-free lattice parameter across both types of EB welded plate derived from neutron diffraction measurements on the 2mm thick strips (described earlier). No distinction was made between stress-free lattice parameter measurements from the two instrument detector banks or with measurement orientation as no systematic variation was observed. Despite a large

degree of scatter in the results (Figure 2), a correlation with the martensitic zone and HAZ boundaries (± 0.8mm and ± 1.35mm respectively) is evident. The greater values of lattice parameter in the martensitic zone, and to a lesser extent in the HAZ, may be attributed to the lattice being supersaturated with carbon. The stress-free lattice spacing measurements at 1.5mm from the weld centre-line and beyond, show little scatter; these data represent parent material unaffected by the welding process. The idealised line in this region (see Figure 2) is based on the mean of all "stress-free" measurements made in parent material; that is in the 2mm strips, at the remote ends of the plates and in small parent cuboids. Stress-free lattice parameter measurements through the thickness in the fusion zones of the 2mm thick strips show a large scatter that appears to be random. For this reason all the lattice spacing measurements made with gauge volumes either fully immersed or partially within the martensitic transformed zone, that is within ±0.75mm of the weld centreline, have been averaged to give a single martensitic weld metal value for use in the strain and stress calculations. A linear variation in stress-free lattice parameter from the average weld to average parent values is assumed in the HAZ. This idealised variation in reference lattice parameter across the welds is marked in Figure 2.

Figure 3(a) shows the distributions of residual stress acting in the longitudinal, transverse and normal directions measured by neutron diffraction across the single pass plate EB weld centre-line at 1.5 mm below the top surface. The longitudinal stress profile exhibits an 'M' shape having tensile peaks of about 475 MPa magnitude that are almost symmetric about the weld centre-line and roughly coincide with the maximum extent of the HAZ. Interestingly the stresses are much lower in a central zone 1.5 mm wide that spans the weld centre-line. The width of this zone correlates exactly with the weld martensitically transformed region (plateau) revealed by the hardness profile of Figure 1(c). The normal component of residual stress has lower magnitude but follows the same profile as the longitudinal component, whereas the transverse stress varies smoothly across the weld apart from one point (at -1.0 mm) that may be an experimental anomaly.

The corresponding measured distributions of residual stress in the EB welded plate with the smoothing pass are shown in Figure 3(b). Again the longitudinal stress profile exhibits an 'M' shape with a tensile peak stress approaching 500 MPa. But in this test specimen the minimum stress appears to be displaced 1 mm from the notional centre-line of the first EB weld pass. This shift could be associated with a lateral offset in the position of the smoothing pass relative to the first pass, or measurement positioning error, or a combination of the two effects. Like the single EB weld the longitudinal stresses rise rapidly in the HAZ, but here the high tensile region is significantly (1.5 mm) wider. Both the normal and transverse components of residual stress have lower magnitude than the longitudinal component but follow the same shape.
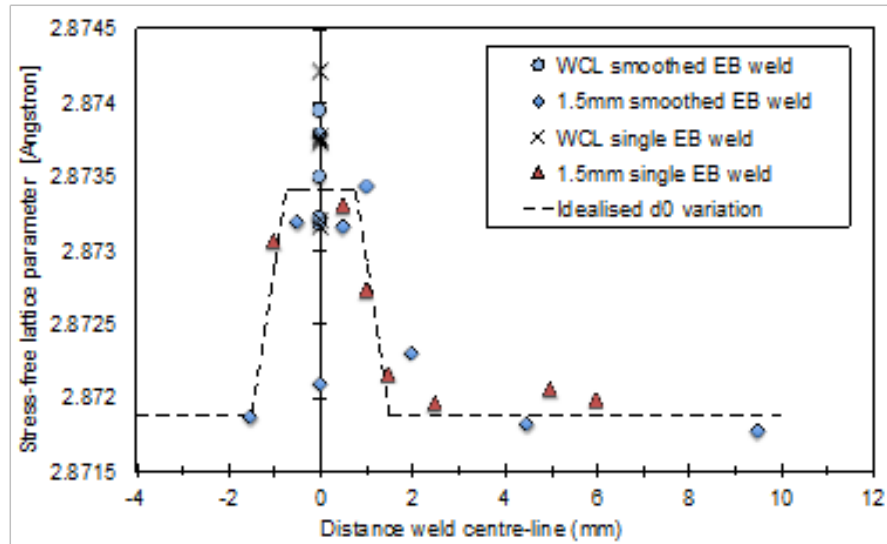
**Figure 2.**  Stress-free lattice parameter variation along the weld centre-line measured by neutron diffraction in both the single EB weld and two pass smoothed EB welds



(a)



(b)
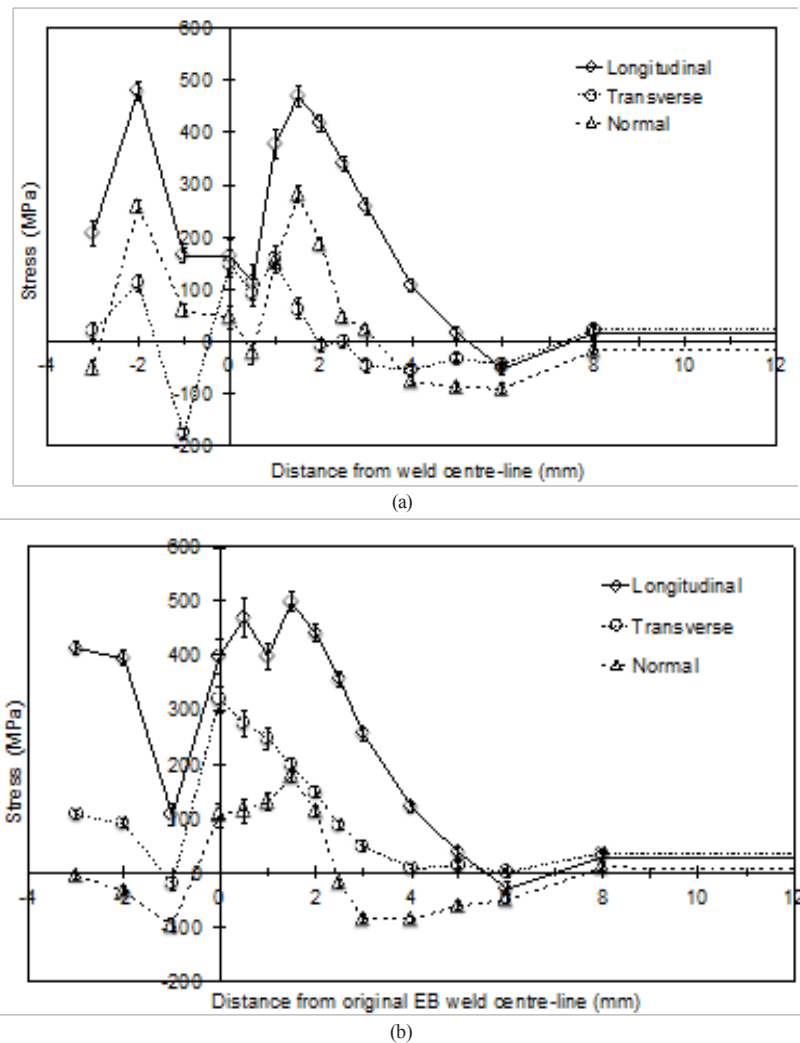
**Figure 3.**  Residual stress distributions in the as-welded plates at 1.5 mm below the top surface measured by neutron diffraction; (a) the single pass EB weld and (b) the two pass smoothed weld

The stresses acting through the thickness of the single pass EB weld are shown in Figure 4(a). The most notable feature of these profiles is the low tensile magnitude in the longitudinal direction and the compressive nature of the normal stress profile.

The corresponding results for the smooth weld test specimen are shown in Figure 4(b). The magnitudes of the stresses are higher for this case in the top 3 mm of the plate thickness; this is because stresses are being sampled in material adjacent to the martensitic zone of the smoothing pass. Interestingly the stresses profiles from 4 to 9 mm below the top surface from the two welds closely match each other. This evidence suggests that neutrons have sampled the lower part of the main EB weld fusion zone in both plates. Although the smooth variations in measured stress through the wall gives confidence in these results, the weld metal measurements have high uncertainty owing to the observed scatter in stress-free reference measurements (Figure 2).



(a)



(b)
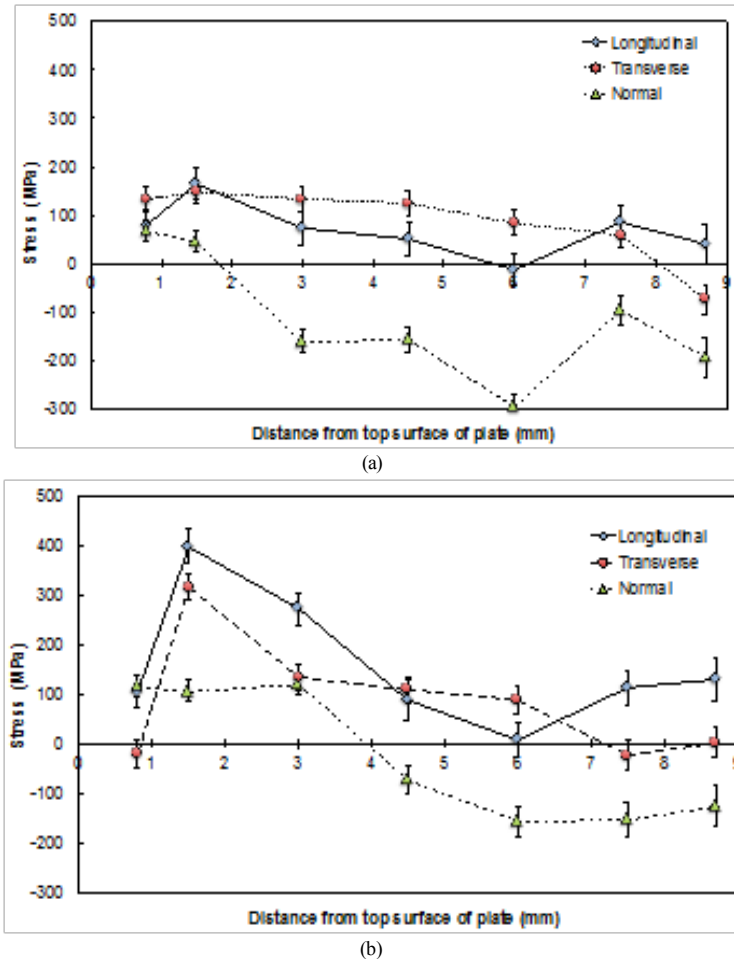
**Figure 4.** Measured residual stress distribution through the thickness weld at the weld centre-line (a) the single pass EB weld and (b) the two pass smoothed weld

As expected the highest tensile stresses across the EB welded joints are in the longitudinal orientation, since this is the direction that is exposed to the highest contraction strain as a consequence of the welding thermal cycle. The second highest tensile stresses are in the normal direction. This is unusual because the magnitude of the normal stress component is usually low in conventional fusion weldments. The normal stresses are greater than the transverse for an EB weld because the weld fusion width to depth aspect ratio is very small ($\approx 0.1$) whereas for a conventional weld bead this ratio is usually greater than unity.

The most striking feature of both M-shaped cross-weld stress profiles is that stresses close to the weld centre-line are significantly less tensile than at the HAZ boundary and in the parent plate material beyond. This feature can arise in steels that undergo a solid state phase transformation from austenite upon cooling to bainite and martensite[1, 5, 6]. It is

notable that the low stresses coincide exactly with the extent of the high hardness plateau shown in Figures 1(a) for the single pass EB weld and Figure 1 (b) for the two pass (smoothed) EB weld, that characterises the extent of the martensitic zone created during cool-down. Reduced levels of residual stress in martensitically transformed regions of multi-pass P91 weldments have been predicted by[5] and measured by Yaghi et al[7] using X-ray diffraction. More recently a zone of compression associated with the final weld bead deposit of a multi-pass weld in a P91 pipe has been measured by the contour method[3] and also by neutron diffraction[3] with the latter study specifically linking the compressive region to martensitic transformation. The current results are also broadly consistent with those of Francis et al.[1] for a single weld bead deposited on a 20 mm thick plate made of SA508 steel, and Dai et al[8] who interrogated low transformation temperature groove welds in

12 mm thick plates. In both of these cases the low stress region extended throughout the fused region into the HAZ and this appeared "to push" highest tensile stresses laterally outwards towards and beyond the HAZ/parent material boundary.

The potential for development of flaws during cooling after welding (e.g. hydrogen cracking), and the development of low toughness microstructures in either the weld metal or HAZ are of significant concern during fabrication and for safe life management. In P91 steel the toughness of the fine grained HAZ is a particular concern as this region is susceptible to type IV cracking[1, 3] when exposed to load at high temperature. The present measurements show that high tensile triaxial residual stresses are generated by the EB welding process in the Type IV region. Of course, P91 weldments are always post weld heat treated (PWHT) prior to engineering use for metallurgical reasons and this treatment can be effective in relieving high levels of residual stress introduced by welding. But Paddea et al.[3] has reported hydrostatic stresses of up to 100 MPa remaining in the Type IV zone of a conventional multi-pass pipe butt weld after PWHT.

Residual stress fields that vary rapidly over fine length-scales are difficult to measure with high reliability. Here special care was taken to use a small gauge volume ($1\,mm^3$) – at the expense of longer acquisition times, position the sample and reference strips to within tens of microns using theodolites and select appropriately spaced measurement locations. The measured results are suitable for validating finite element prediction of residual stresses in electron beam welded plates, although more detailed information from other techniques such as the Contour method[9] is desirable to confirm full field predictions.

# 4. Conclusions

Residual stresses in 9 mm thick EB welded plates have been measured using neutron diffraction. A characteristic 'M-shape' distribution of stresses across the weld line has been observed with high tensile peaks situated just beyond the HAZ/parent material boundary in both the single pass and two pass EB welded plates, that is immediately outside those regions that have either fully or partially austenitised during welding. The length-scale of this stress distribution is very short with the tensile peaks approximately 3 mm apart spanning a 1 mm wide fused zone. Measured stresses close to the weld centre-line are significantly less tensile than the adjacent peaks owing to martensitic solid state phase transformation during cool-down of fused weld metal and adjacent austenitised material within the HAZ. Residual stresses in the EB welded plate with a second smoothing pass have higher tensile magnitude and greater spread than the single pass case. Therefore from a residual stress and structural integrity point of view application of a smoothing (second) EB weld pass is undesirable.

# REFERENCES

[1]  Francis JA, Mazur W, Bhadeshia HKDH, Materials Science and Technology, Vol. 22, 2006, p. 1387.

[2]  Haarmann JC, Vallant B, Vandenberghe W, Bendrick AA, The T91/P91 Book, 2nd edn. Vallourec & Mannesmann Tubes, 2002.

[3]  Paddea S, Francis JA, Paradowska AM, Bouchard PJ, Shibli IA, Materials Science and Engineering A, 2012, Accepted.

[4]  Von Dreele RB, Jorgensen J, Windsor CG, Journal of Applied Crystallography, 1982, p. 581.

[5]  Yaghi AH, Hyde TH, Becker A, Sun W, Journal of Strain Analysis, Vol. 43, 2008, p. 275.

[6]  Francis JA, Turski M, Withers PJ, Materials Science and Technology, Vol.25, 2009, p. 325.

[7]  Yaghi AH, Hyde TH, Becker A, Sun W, Science and Technology of Welding and Joining, Vol. 16, 2011, p. 232.

[8]  Dai H, Francis JA, Stone HJ, Bhadeshia HKDH, Withers PJ, Metallurgical and Materials Transactions A, Vol. 39A, 2008, p. 3070.

[9]  Prime MB, Journal of Engineering Materials and Technology, Vol. 123, 2001, p. 162.